FULL TITLE
ASP Conference Series, Vol. **VOLUME**, **YEAR OF PUBLICATION**
NAMES OF EDITORS

arXiv:0811.0472v1 [astro-ph] 4 Nov 2008

Supergranulation Scale Connection Simulations

Robert F. Stein[1], Åke Nordlund[2], Dali Georgoviani[1], David Benson[3], Werner Schaffenberger[1]

Abstract. Results of realistic simulations of solar surface convection on the scale of supergranules (96 Mm wide by 20 Mm deep) are presented. The simulations cover only 10% of the geometric depth of the solar convection zone, but half its pressure scale heights. They include the hydrogen, first and most of the second helium ionization zones. The horizontal velocity spectrum is a power law and the horizontal size of the dominant convective cells increases with increasing depth. Convection is driven by buoyancy work which is largest close to the surface, but significant over the entire domain. Close to the surface buoyancy driving is balanced by the divergence of the kinetic energy flux, but deeper down it is balanced by dissipation. The damping length of the turbulent kinetic energy is 4 pressure scale heights. The mass mixing length is 1.8 scale heights. Two thirds of the area is upflowing fluid except very close to the surface. The internal (ionization) energy flux is the largest contributor to the convective flux for temperatures less than 40,000 K and the thermal energy flux is the largest contributor at higher temperatures. This data set is useful for validating local helioseismic inversion methods. Sixteen hours of data are available as four hour averages, with two hour cadence, at steinr.msu.edu/∼bob/96averages, as idl save files. The variables stored are the density, temperature, sound speed, and three velocity components. In addition, the three velocity components at 200 km above mean continuum optical depth unity are available at 30 sec. cadence.

1. The Simulation

Solar surface convection on supergranular scales (96 Mm wide by 20 Mm deep) was simulated by solving the conservation equations for mass, momentum and internal energy. Spatial derivatives were evaluated using sixth order finite differences (Nagarajan, Lele & Ferziger 2003) and the time advance was by a low memory, third order Runge-Kutta scheme (Kennedy, Carpenter & Lewis 1999). The calculations were performed on a grid of $1000^2 \times 500$ giving a resolution of 96 km horizontally and 12-70 km vertically. f-plane rotation is included corresponding to a latitude of 30.

A tabular equation of state which includes local thermodynamic equilibrium (LTE) ionization of the abundant elements as well as hydrogen molecule formation, was used to obtain the pressure and temperature as a function of log density and internal energy per unit mass. The radiative heating/cooling

[1]Michigan State University, East Lansing, MI 48824, USA

[2]Niels Bohr Institute, Copenhage, DK-2500, DK

[3]Kettering University, Flint, MI

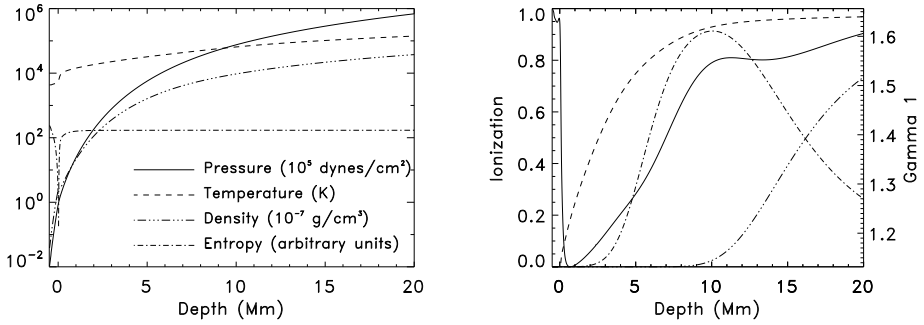

Figure 1. Pressure, temperature, density, entropy (left), Gamma1 (solid), H ionization fraction (dashed), and He ionization fractions (dash dot and dast dot dot dot) (right). The computational domain covers 10 % of the geometric depth of the solar convection zone and half its scale heights. There are 5 orders of magnitude in pressure, four in density and one in temperature within the convective region included.

was obtained by solving the radiation transfer equation in both continua and lines using the Feautrier method, assuming Local Thermodynamic Equilibrium (LTE). The number of wavelengths for which the transfer equation is solved is drastically reduced by using a multi-group method whereby the opacity at each wavelength is placed into one of four bins according to its magnitude and the source function is binned the same way (Nordlund 1982; Stein & Nordlund 2003).

Horizontal boundary conditions are periodic, while top and bottom boundary conditions are open. The code is stabilized by diffusion in the momentum and energy equations, using a variable diffusivity that depends on the sound speed, the fluid velocity and the compression.

2. The Atmosphere

The computational domain covers five orders of magnitude in pressure in the convective region, which is half the scale heights in the entire solar convection zone, even though the domain is only 10% of the zones geometric depth (Fig. 1). This includes the hydrogen ionization layer and the first and most of the second helium ionization layers. A shear layer develops with a shear of 100 m/s across the 20 Mm depth of the domain.

Convective motions are turbulent. Descending vortex rings have typical mushroom shape and are connected back to surface with multiple twisted vortex tubes (Fig. 2). The horizontal scale of the convection increases from granule size at the surface to supergranule size near the bottom of the computational domain (Fig. 3). The horizontal velocity spectrum at the surface is a power law, with the magnitude of the velocity decreasing linearly with increasing size. There is a peak at granule scales and then a fall off at still smaller scales. About 2/3 of the area is upflows and 1/3 downflows nearly independent of depth.

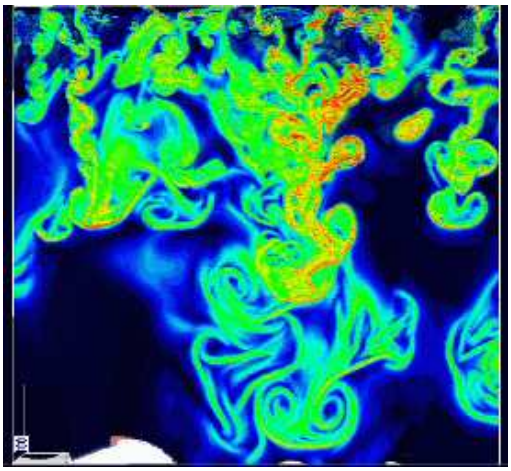

Figure 2. Finite time (11.75 hours) Lyapunov exponent field ov a subdomain 21 Mm wide by 19 Mm high, by 0.5 Mm thick, from a 48 wide × 20 Mm deep simulation. This corresponds closely to the magnitude of the vorticity. Figure courtesy Bryan Green, AMTI/NASA.

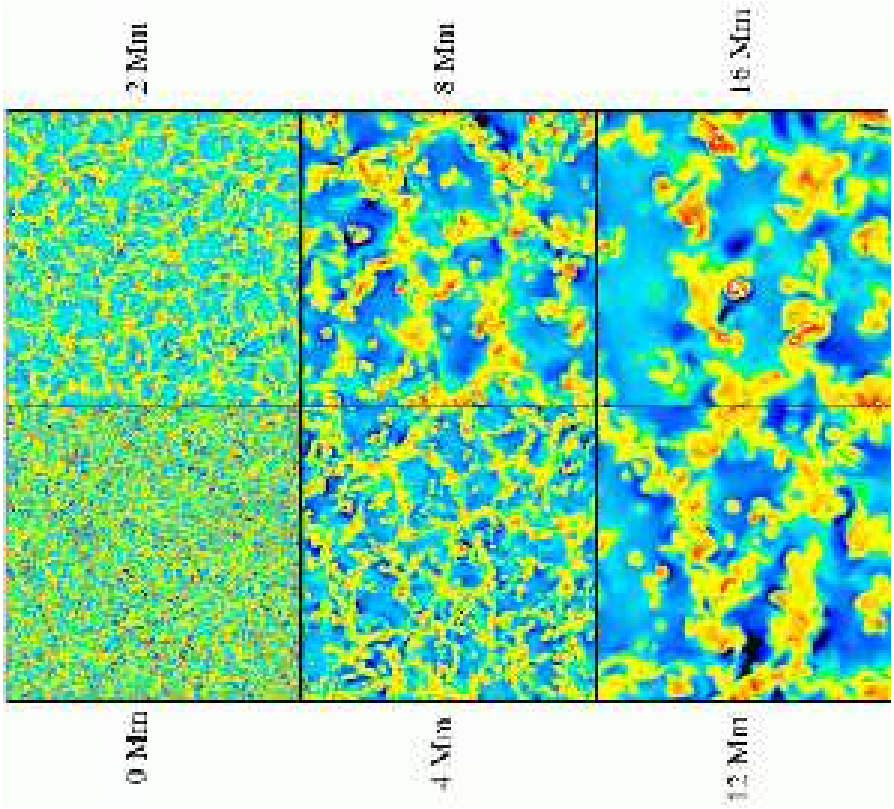

Figure 3. Vertical velocity on horizontal slices at the surface and 2, 4, 8, 12, and 16 Mm below the surface. Red and yellow are downflows. Blue and green are upflows. The dominant horizontal scale of the convection increases monotonically with increasing depth.

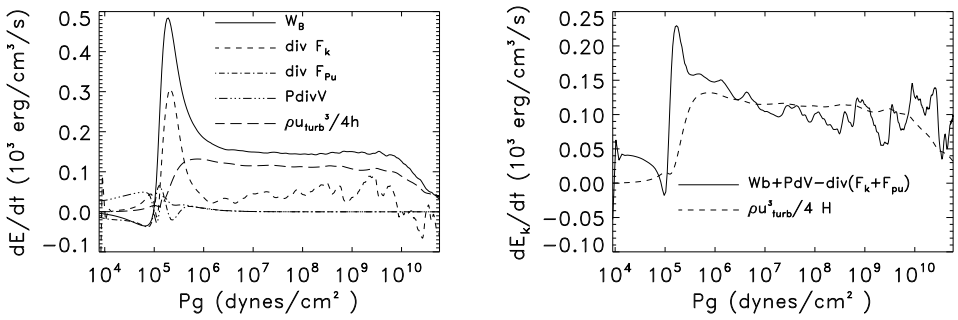

Figure 4. Contributions to the kinetic energy equation. Most of the buoyancy driving occurs just below the surface where the entropy fluctuations are large, but remains significant and nearly constant at larger depths. The buoyant work is balanced by the divergence of the kinetic energy flux near the surface and by dissipation in the interior. The change in behavior near the bottom boundary is due to boundary condition effects and is not physical.

3. Driving and Damping

Convection on the Sun is driven primarily by radiative cooling in a thin boundary layer at the bottom of the photosphere where radiation begins to escape to space. Radiative cooling produces low entropy, over dense fluid that is pulled down by gravity. There is also driving from the bottom of the convection zone where absorption of the radiative flux heats the fluid producing high entropy, under dense fluid. However, the entropy fluctuations near the surface are much much larger than those near the bottom of the convection zone, so most of the buoyant work occurs near the surface (Fig. 4). The buoyancy driving is balanced by the divergence of the kinetic energy flux close to the surface and by dissipation at small scales through the remainder of the convection zone. The damping length is 4 pressure scale heights (Fig. 4).

4. Energy Fluxes

Most of the energy in the cooler part of the convection zone close to the surface where hydrogen is partially ionized is carried by the internal (ionization) energy flux. At temperatures above 40,000 K, this decreases and most of the energy is transported by the thermal energy flux (Fig. 5).

5. Mixing Length

The mass mixing length is the inverse of the logarithmic derivative of the unidirectional (either up or down) mass flux, $\ell = (dF_{\rm mass}(down)/dr/F_{\rm mass}(down))^{-1}$. Figure 5 shows that over most of the computational domain except right near the surface the mass mixing length is 1.8 pressure scale heights. This is an easy, unambiguous, calculation to make for other stars as well to determine the appropriate mixing length.

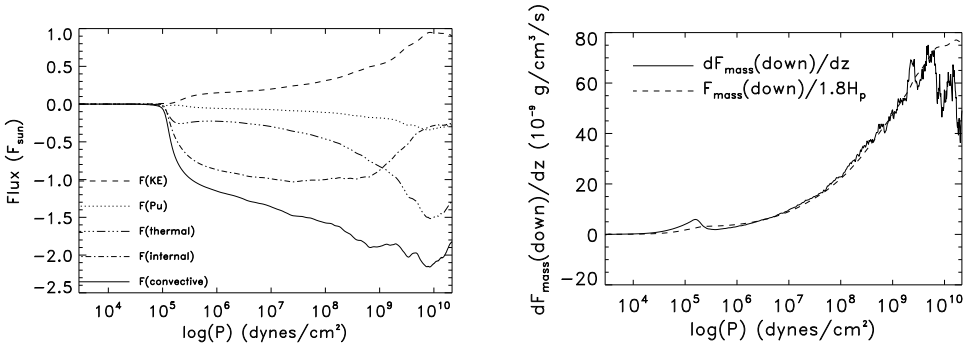

Figure 5. Energy fluxes (left) and mass mixing length (right). Note negative fluxes are upward energy transport. The kinetic energy flux is downward and approximately half the magnitude of the total other, upward, energy fluxes. Energy is transported primarily as the internal (ionization) energy below 40,000 K and primarily as the thermal energy at higher temperatures. Upflowing fluid turns over and is entrained in the downflows in order to conserve mass with a length scale or mixing length of 1.8 pressure scale heights.

6. Application to Local Helioseismology

Sixteen hours of data are available as four hour averages, with two hour cadence, at steinr.msu.edu/∼bob/96averages, as idl save files. The variables stored are the density, temperature, sound speed, three velocity components. In addition, the three velocity components at 200 km above mean continuum optical depth unity are available at 30 sec. cadence.

7. Summary

A realistic simulation of supergranulation scale convection, covering half the scale heights in the solar convection zone can be used to evaluate local helioseismic inversion proceedures. It has also allowed us to determine the mass mixing length (1.8 H_P), to show that most of the energy is transported as ionization energy below 40,000 K and as thermal energy above that temperature, and that the buoyancy driving is largest close to the surface, but significant throughout the simulated domain. In the interior, this driving is balanced primarily by dissipation at small scales and the damping length is 4 H_P. Four hour averages with two hour candence of the density, temperature, sound speed, and three velocity components are available as idl save files. In addition, the three velocity components at 200 km above mean continuum optical depth unity are available at 30 sec. cadence.

Acknowledgments. The calculations were performed at the NASA High End Computing Columbia supercomputer. Support for this project was provided by NASA grants NNX07AO71G, NNX07AH79G, NNX07AI08G and NNX08AH44G, and NSF grant AST 0605738. This support is greatly appreciated.

References

C. A. Kennedy, M. H. Carpenter, & R. M. Lewis 1999, ICASE Report No. 99-22, NASA/CR-1999-209349
S. Nagarajan, S. K. Lele & J. H. Ferziger 2003, J. Comp. Phys., 191, 392–429
Å. Nordlund, Astron. & Astrophys. 1982, 107, 1–10
R. F. Stein and Å. Nordlund 2003, in Stellar Atmosphere Modeling, eds. I. Hubeny, D. Mihalas and K. Werner, ASP Conf. Proc. 288, 519–532